Journal of General Virology (2015), **96**, 3507–3518 **DOI** 10.1099/jgv.0.000306

Employing transposon mutagenesis to investigate foot-and-mouth disease virus replication

Morgan R. Herod,[1] Eleni-Anna Loundras,[1] Joseph C. Ward,[1] Fiona Tulloch,[2] David J. Rowlands[1] and Nicola J. Stonehouse[1]

Correspondence
Nicola J. Stonehouse
n.j.stonehouse@leeds.ac.uk

[1]School of Molecular and Cellular Biology, Faculty of Biological Sciences and Astbury Centre for Structural Molecular Biology, University of Leeds, Leeds LS2 9JT, UK

[2]Biomedical Sciences Research Complex (BSRC), School of Biology, University of St Andrews, North Haugh, St Andrews, KY16 9ST, UK

Received 17 July 2015
Accepted 30 September 2015

Probing the molecular interactions within the foot-and-mouth disease virus (FMDV) RNA replication complex has been restricted in part by the lack of suitable reagents. Random insertional mutagenesis has proven an excellent method to reveal domains of proteins essential for virus replication as well as locations that can tolerate small genetic insertions. Such insertion sites can subsequently be adapted by the incorporation of commonly used epitope tags, facilitating their detection with commercially available reagents. In this study, we used random transposon-mediated mutagenesis to produce a library of 15 nt insertions in the FMDV non-structural polyprotein. Using a replicon-based assay, we isolated multiple replication-competent as well as replication-defective insertions. We adapted the replication-competent insertion sites for the successful incorporation of epitope tags within FMDV non-structural proteins for use in a variety of downstream assays. Additionally, we showed that replication of some of the replication-defective insertion mutants could be rescued by co-transfection of a 'helper' replicon, demonstrating a novel use of random mutagenesis to identify intergenomic *trans*-complementation. Both the epitope tags and replication-defective insertions identified here will be valuable tools for probing interactions within picornavirus replication complexes.

INTRODUCTION

Foot-and-mouth disease is an acute systemic disease of cloven-hoofed animals, outbreaks of which in domestic livestock have significant economic consequences for the agricultural and tourism industries. The causative agent, foot-and-mouth disease virus (FMDV), is endemic in wide areas of Asia, Southern America, Africa and the Middle East and has the potential to cause major epidemics globally. Difficulties arising from the control of the spread of disease stem primarily from the high infectivity and transmissibility of the virus and the asymptomatic carrier state that the virus can adopt.

FMDV is a member of the family *Picornaviridae*, comprising positive-sense ssRNA viruses. The genome is translated as a single ORF, flanked by both 5′ and 3′ UTRs and a 3′ poly(A) tail (Carrillo *et al.*, 2005). The long and highly secondary structured 5′ UTR contains at least five discrete domains, including the type II viral internal ribosome entry site (Belsham & Brangwyn, 1990; López de Quinto & Martínez-Salas, 1997; López de Quinto *et al.*, 2002) and *cre* or *cis*-acting replicative element (Mason *et al.*, 2002) in addition to three elements of unknown function: varying copies of pseudoknots, a polypyrimidine (pC) tract of variable length and a predicted large 5′ stem–loop or S-fragment (Carrillo *et al.*, 2005; Clarke *et al.*, 1987; Escarmís *et al.*, 1995; Mason *et al.*, 2003; Rowlands *et al.*, 1978). The comparatively smaller 3′ UTR contains two stem–loop structures, both of which appear to have roles in viral RNA replication (Rodríguez Pulido *et al.*, 2009; Sáiz *et al.*, 2001).

Following translation, the FMDV polyprotein is processed co- and post-translationally to produce four primary products: mature L^{pro} (self-processed *in cis* at its own C terminus) and the precursors P1–2A, 2BC and P3 ($3AB_{1-3}CD$). Processing at the 2A2B boundary occurs co-translationally through a ribosome skipping mechanism to release P1–2A from the rest of the polyprotein (de Felipe *et al.*, 2003; Donnelly *et al.*, 2001; Ryan & Drew, 1994). The P1–2A primary product is subsequently processed by the 3C/3CD protease to generate three structural proteins, 1AB, 1C and 1D (1AB being cleaved by an unknown mechanism into 1A and 1B in a final virus maturation step), whereas the 2BC and P3 precursors undergo 3C/3CD-mediated proteolysis to generate the mature viral RNA replication proteins (reviewed by Ryan & Flint, 1997). In poliovirus

Four supplementary figures are available with the online Supplementary Material.

and FMDV, non-structural (NS) proteins 2B and 2C along with their precursor 2BC are involved in disrupting endoplasmic reticulum-to-Golgi transport to inhibit the cellular secretory pathway (Doedens & Kirkegaard, 1995; Moffat *et al.*, 2005, 2007) via a PI4K-independent mechanism in FMDV (E. A. Loundras, M. R. Herod, M. Harris and N. J. Stonehouse, unpublished data). The 2C protein from poliovirus also demonstrates ATPase activity and is likely to play a direct role in replicating the viral genome (Rodríguez & Carrasco, 1993; Xia *et al.*, 2015).

The P3 precursor undergoes proteolysis, probably through both major and minor pathways, to generate four mature viral NS proteins: the viral RNA-dependent RNA polymerase $3D^{pol}$ (Ferrer-Orta *et al.*, 2004, 2006, 2009), the major viral protease $3C^{pro}$ (Birtley *et al.*, 2005; Grubman *et al.*, 1995), three non-identical tandem repeats of the primer polypeptide 3B ($3B_{1–3}$) (Forss & Schaller, 1982; King *et al.*, 1980; Nayak *et al.*, 2005; Paul *et al.*, 1998, 2003) and the transmembrane protein 3A (González-Magaldi *et al.*, 2012, 2014). Replication of the viral genome requires expression of all viral NS proteins in addition to *cis*-acting RNA elements, which are thought to localize to membrane-associated replication compartments where viral RNA synthesis occurs. To date, defining the molecular interactions in these replication compartments has largely remained elusive, in part due to the limited reagents available for studying such interactions.

Random transposon-mediated mutagenesis has been exploited extensively for the functional profiling of viral proteins and identifying essential protein functional domains, as well as for characterizing *cis*-acting RNA replication elements (Brune *et al.*, 1999; McMahon *et al.*, 1998; Möhl *et al.*, 2010; Remenyi *et al.*, 2014; Teterina *et al.*, 2011a; Thorne *et al.*, 2012). This powerful technique allows the simultaneous screening of the effect of large numbers of insertional mutations on virus replication to identify locations within proteins that can tolerate small genetic insertions. Once identified, these insertion sites can be utilized for the genetic incorporation of epitope tags, facilitating further downstream studies such as co-immunoprecipitation and immunofluorescence (Teterina *et al.*, 2010, 2011b; Thorne *et al.*, 2012).

In this study, our aim was to use transposon mutagenesis on the FMDV P2P3 polyprotein to identify locations within NS proteins that could tolerate small genetic insertions. For this work, we employed an FMDV replicon, a self-replicating mini viral genome in which the viral structural proteins have been removed and replaced by a reporter transgene allowing quantification of virus replication in the absence of virion production (Tulloch *et al.*, 2014). Using this replicon-based reporter assay, we identified functionally permissive insertion sites in addition to replication-defective insertions. Additionally, we adapted well-tolerated insertion sites by the incorporation of epitope tags. Finally, we demonstrated that replication-defective insertion sites within the 3A NS protein could be complemented *in trans* by co-transfection with a 'helper' replicon construct.

RESULTS

Transposon mutagenesis of the FMDV NS polyprotein

Multiple studies have demonstrated the use of transposon-mediated random mutagenesis to probe the genomes of positive-strand RNA viruses for sites that can tolerate the insertion of small exogenous sequences (McMahon *et al.*, 1998; Remenyi *et al.*, 2014; Teterina *et al.*, 2011a; Thorne *et al.*, 2012). We used this method to identify regions of the FMDV NS polyprotein that can tolerate genetic insertions. The FMDV replicon plasmid pGFP-PAC (Tulloch *et al.*, 2014) was used to generate a replicon library containing insertions solely in the NS polyprotein (2A through to $3D^{pol}$). To exclude irrelevant insertion sites within the vector backbone, the *Xma*I–*Bam*HI fragment of the FMDV NS polyprotein was subcloned into *Xma*I/*Bam*HI-digested pUC18 to generate pUC-2A-3D. Mutagenesis was conducted on pUC-2A-3D prior to replacement of the *Xma*I–*Bam*HI fragment into pGFP-PAC and the transposon was removed from the library by digestion with *Not*I. This resulted in a library of 15 nt insertions spanning the FMDV 2A–3D region. Each 15 nt insertion consisted of 10 nt remaining from the transposon insertion (including a unique *Not*I restriction enzyme site) and 5 nt originating from the target DNA directly upstream of the insertion site, which is duplicated during the transposition event.

To identify insertion sites, *in vitro*-transcribed RNA from the transposon-mutated replicon library was transfected into BHK-21 cells along with appropriate controls. Transfection was performed with 0.3 or 1 μg of *in vitro*-transcribed RNA per well. Total RNA was extracted at 8 h post-transfection when GFP expression was maximal (Fig. S1, available in the online Supplementary Material), replicon genomes were amplified by reverse transcription PCR (Fig. S2) and subcloned into a plasmid vector. To identify a limited selection of different transposon insertions, a total of 38 individual clones were selected at random and the location of the transposon insertions were determined by DNA sequencing. The name of each transposon insertion was derived from the nucleotide of the corresponding NS protein after which the insertion occurred (Tables 1 and 2).

Of the 16 clones isolated from transfection of 0.3 μg RNA, 11 insertions were located in the C-terminal region of 3A, downstream of the predicted transmembrane region. Two insertion sites were within the multiple copies of 3B (one within $3B_1$ and one within $3B_2$), with two insertions in 2C and one within the $3D^{pol}$ coding region. Similarly, of the 22 clones isolated after transfection of 1 μg of the transposon library, seven insertions were in 3A, with one

Table 1. Transposon insertions identified after selection following transfection with 0.3 μg of replicon library RNA

All transfections used 0.3 μg of replicon library RNA. The location of each insertion identified is named with a number indicating the nucleotide residue of the corresponding FMDV NS protein after which the insertion occurred. The dinucleotide at which insertion occurred is shown in bold. The inserted nucleotide sequence and amino acid translation are underlined.

Name	Insertion site	Nucleotide insertion	Amino acid sequence
2C17	CA**TC**AA	**T**CAACTGCGGCCGCAT**C**	KARDINCGRINDIFA
2C842	CA**AG**AC	**A**GACTGCGGCCGCAAA**G**	KRMQQDCGRKDMFKP
3A229	TC**CG**TG	**C**GTTGCGGCCGCATCC**G**	IVIMIRCGRIRETRK
3A233	TG**AG**AC	**A**TGCGGCCGCACGTGA**G**	VIMIRDAAARETRKR
3A266	TG**CA**GT	**C**AGTGCGGCCGCATGC**A**	MVDDAVRPHAVNEY
3A274	AT**GA**GT	**G**AGTTGCGGCCGCATG**A**	DAVNELRPHEYIEKA
3A282	TT**GA**GA	**G**ATGCGGCCGCAATTG**A**	VNEYIDAAAIEKANI
3A339	CC**TC**TA	**T**CTATGCGGCCGCACT**C**	AEKSPLCGRTLETSG
3A342	TA**GA**GA	**G**AGATGCGGCCGCAAG**A**	EKSPLEMRPQETSGA
3A350	AG**CG**GC	**C**GGCTGCGGCCGCAGC**G**	SPLETSGCGRSGAST
3A354	GC**GC**CA	**G**CCAGCTGCGGCCGCA**C**	ETSGASCGRTSTVGF
3A387	TC**CC**AG	**C**CAGTGCGGCCGCACC**C**	RERTLPVRPHPGQKA
3A442	AG**GA**GC	**G**TGCGGCCGCATGAGG**A**	QPVEVRPHEEQPQ
$3B_1$7	CC**TA**CG	**T**ACGCTGCGGCCGCAT**A**	EGPYAAAAYAGPLE
$3B_2$25	GA**GA**CA	**G**ACTGCGGCCGCAGAG**A**	AGPMERLRPQRQKPL
3D450	AT**GG**AG	**G**GATGCGGCCGCAATG**G**	ALKLMDAAAMEKREY

Table 2. Transposon insertions identified after selection following transfection with 1 μg of replicon library

All transfections used 1 μg of replicon library RNA. The location of each insertion identified is named with a number indicating the nucleotide residue of the corresponding FMDV NS protein after which the insertion occurred. The dinucleotide at which insertion occurred is shown in bold. The inserted nucleotide sequence and amino acid translation are underlined.

Name	Insertion site	Nucleotide insertion	Amino acid sequence
3A229	TC**CG**TG	**C**GTTGCGGCCGCATCC**G**	IVIMIRCGRIRETRK
3A234	TG**AG**AC	**A**GTGCGGCCGCAGTGA**G**	IMIRECFRSETRKRM
3A301	CC**AC**AG	**A**CAGTGCGGCCGCACA**C**	KANITTVRPHTDDKT
3A303	CA**CA**GA	**C**AGATTGCGGCCGCAC**A**	ANITTDCGRTDDKTL
3A339	CC**TC**TA	**T**CTATGCGGCCGCACT**C**	AEKSPLCGRTLETSG
3A341	CT**CT**AG	**C**TAGTGCGGCCGCATC**T**	AEKSPLVRPHLETSG
3A358	CC**AG**CA	**A**GTGCGGCCGCAGCCA**G**	TSGASAAAASTVGFR
$3B_1$11	CG**CC**GG	**C**CGGATGCGGCCGCAC**C**	EGPYAGCGRTGPLER
$3B_3$11	GA**GG**GA	**G**GGTGCGGCCGCAGAG**G**	EGPYEGAAAEGPVKK
3C1	TG**AG**AG	**A**GTGCGGCCGCACTGA**G**	KNLIVTECGRTESGA
3C57	GT**TG**AG	**T**GAGTGCGGCCGCATT**G**	NTKPVECGRIELILD
3C196	AG**TG**AC	**T**GACTGCGGCCGCAGT**G**	AMTDSDCGRSDYRVF
3C319	AC**AG**CA	**A**GCTGCGGCCGCAACA**G**	KHFDTAAAATARMKK
3D306	AT**CA**AG	**C**AAGTGCGGCCGCATC**A**	IYEAIKCGRIKGVDG
3D489	CT**GA**AG	**G**AATGCGGCCGCACTG**A**	CQTFLNAAALKDEIR
3D525	CC**GG**TA	**G**GTGCGGCCGCAGCCG**G**	EKVRAGAAAAGKTRI
3D651	TG**CA**AC	**C**AACTGCGGCCGCAGC**A**	SAVGCNCGRSNPDVD
3D657	CC**CT**GA	**C**TGATTGCGGCCGCAC**T**	VGCNPDCGRTDVDWQ
3D716	GG**AC**TA	**A**TGCGGCCGCAGTGGA**C**	WDVDAAAVDYSAFD
3D738	GC**TA**AT	**T**AATGCGGCCGCAGCT**A**	SAFDANAAAANHCSD
3D747	TG**TA**GT	**T**AGTTGCGGCCGCAGT**A**	DANHCSCGRSSDAMN
3D750	TA**GT**GA	**G**TTGCGGCCGCAGTAG**T**	ANHCSCGRSSDAMNI

insertion in $3B_1$ and $3B_3$, respectively. In addition, using this higher RNA concentration, four and nine insertions were identified in $3C^{pro}$ and $3D^{pol}$, respectively. Only two common insertions were isolated after transfection with either RNA concentration, all within the 3A C-terminal region (3A229 and 3A339).

To broadly screen a selection of the identified transposon insertions for replication competence, 11 3A transposon insertions, one insertion in each of $3B_{1–3}$ and all the isolated 2C, $3C^{pro}$ and $3D^{pol}$ insertions were introduced individually into the pGFP-PAC replicon. RNA transcripts were generated and transfected into BHK-21 cells along with a wt positive control and a replication-defective negative-control construct bearing a large deletion of the polymerase gene ($\Delta 3D^{pol}$), and replication was monitored by GFP expression hourly over a 24 h period using an IncuCyte Dual Colour Zoom FLR. Relative replication is shown at maximal GFP expression at 8 h post-transfection (Fig. 1).

All except one of the replicon constructs containing transposon insertions in 3A demonstrated a replication level above that of the replication-defective polymerase knockout control (indicating the level of input translation), the exception being the insertion at nucleotide 3A341, which was replication-incompetent. All 3B transposon insertions tested also demonstrated replication almost equivalent to the wt construct. The single $3D^{pol}$ insertion identified after transfection of 0.3 μg of RNA from the transposon-mutated replicon library (3D450) replicated to wt levels, whereas none of the $3C^{pro}$ or $3D^{pol}$ insertions identified after transfection of 1 μg of library RNA was replication competent, and only expressed GFP equivalent to the polymerase knockout control construct ($\Delta 3D^{pol}$). Neither of the isolated 2C transposon insertions showed replication in BHK-21 cells. Notably, a limited number of the replicon constructs containing transposon insertions demonstrated GFP expression below that of the negative-control polymerase knockout replicon, in particular insertions 3A341 and 3D747, as well as possibly both 2C insertions.

Modifications of the C-terminal portion of FMDV 3A have been shown to limit replication of the virus in bovine cells (Beard & Mason, 2000; Li *et al.*, 2010; Pacheco *et al.*, 2003, 2013). To investigate whether the identified replication-competent transposon insertions could replicate in bovine cells, replicons bearing replication-competent insertions were transfected into Madin–Darby bovine kidney (MDBK) cells along with controls, and GFP expression was monitored over 24 h (Fig. 2).

The majority of 3A insertions completely eliminated or severely impaired replication in MDBK cells, with the exception of the 3A339, 3A358 and 3A387 insertions, which maintained over 50 % replication. The identified

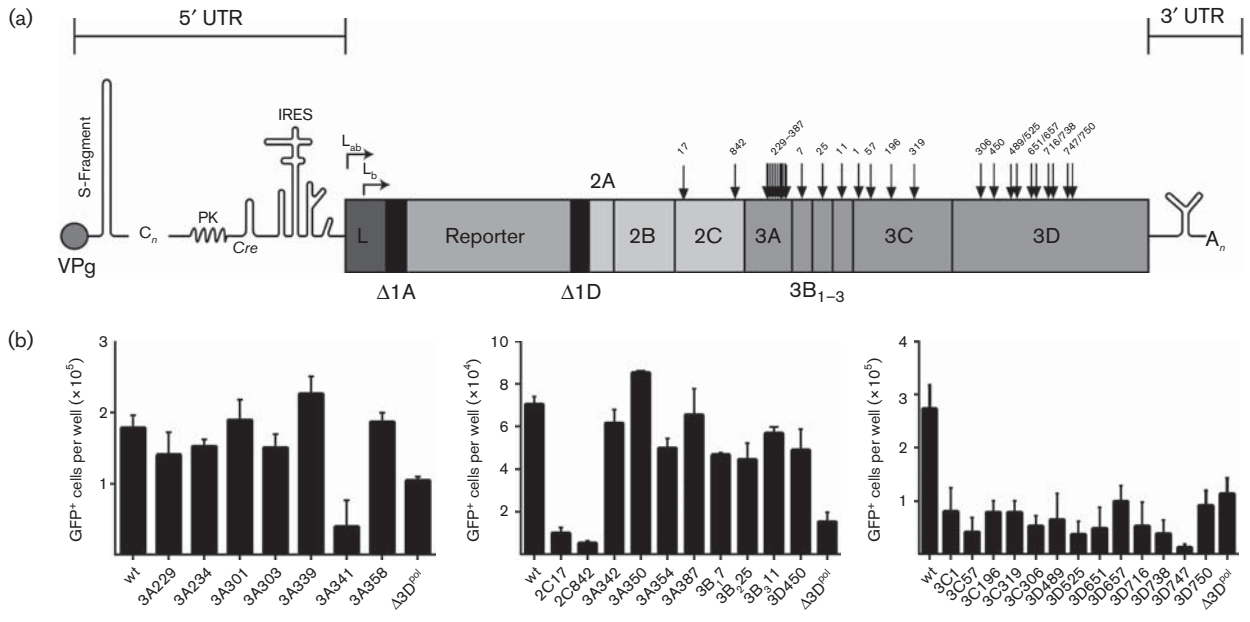

Fig. 1. Replication of individual transposon insertions in BHK-21 cells. (a) Schematic of the FMDV replicon genome showing the location of transposon insertions chosen for analysis. Numbers indicate the nucleotide residue of the corresponding FMDV NS protein after which insertion occurred. (b) BHK-21 cells seeded into 12-well plates were allowed to adhere for 16 h before transfection with replicon transcripts containing individual transposon insertions using Escort reagent. Wt GFP–PAC replicon and polymerase knockout ($\Delta 3D^{pol}$) constructs were included, the latter being a negative control for input translation. GFP expression was monitored hourly using an IncuCyte Zoom Dual Colour FLR and analysed using the integrated software. The data shown represent GFP-positive cells per well at 8 h post-transfection ($n=2$, mean ± SEM).

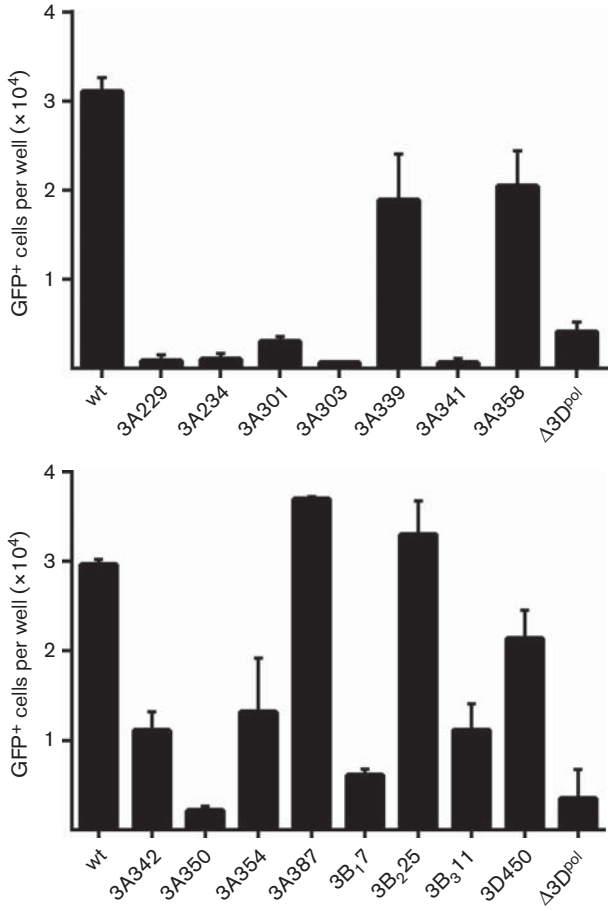

Fig. 2. Replication of individual transposon insertions in MDBK cells. MDBK cells seeded into 12-well plates were allowed to adhere for 16 h before transfection with replicon transcripts containing individual transposon insertions using Escort reagent. Wt GFP–PAC replicon (wt) and polymerase knockout ($\Delta 3D^{pol}$) constructs were included, the latter as a negative control for input translation. GFP expression was monitored hourly using an IncuCyte Zoom Dual Colour FLR and analysed using the integrated software. The data shown represent GFP-positive cells per well at 8 h post-transfection ($n=2$, mean $\pm$ SEM).

transposon insertions in $3B_1$ and $3B_3$ were essentially replication-incompetent in MDBK cells, whereas the $3B_2$ insertion tested maintained replication equal to the wt replicon. The replication-competent $3D^{pol}$ insertion (3D450) maintained good replication in MDBK cells, with GFP expression approximately 50 % of that of the wt replicon.

Generation of tagged FMDV replicons

Identification of replication-competent insertion sites suggests potential locations for insertion of alternative exogenous sequences such as epitope tags. Two frequently used small epitope tags, FLAG (DYKDDDDK) and haemagglutinin (HA; YPYDVPDYA), were chosen for insertion into two different locations in 3A (after nt 303 and 358) and the one functional $3D^{pol}$ insertion site (nt 450) (Fig. 3a), all three insertion sites demonstrating high levels of replication in BHK-21 cells. Insertion site 3A303 was selected for epitope labelling, based on the inserted transposon sequence at this location (DCGRTDDK; Table 2), which partially resembled a FLAG epitope, and 3A358 was selected as this demonstrated moderate replication in MDBK cells. Replication of the epitope-tagged replicon constructs was assessed in both BHK-21 and MDBK cells along with the relevant controls (Fig. 3b, c).

Replicons bearing either a FLAG or an HA tag in any of the 3A insertion sites tested showed levels of replication equivalent to the wt replicon in BHK-21 cells but little or no replication in the bovine cell line MDBK. In contrast, insertion of either epitope tag in the 3D450 insertion site completely abrogated replication, even in BHK-21 cells.

Western blot analysis of BHK-21 cells transfected with FLAG- and HA-labelled 3A replicons using anti-FLAG and anti-HA primary antibodies detected epitope-labelled 3A and 3A precursors as expected (Fig. 3d). Probing with an anti-3A mAb also detected epitope-labelled 3A303 but failed to detect either 3A358FLAG or 3A358HA, possibly because genetic insertions in this position disrupted the epitope recognized by this mAb or because insertion of the epitope tags disrupted the native folding of 3A when introduced into this position.

To demonstrate that the epitope-tagged replicons could be used for immunofluorescent detection of 3A, BHK-21 cells were transfected with the 3A303FLAG or 3A358FLAG replicon, fixed at 8 h post-transfection, probed with an anti-FLAG antibody and analysed by confocal microscopy (Fig. 3e). As anticipated, FLAG staining was clearly detected only in cells expressing the GFP transgene, used as a marker for replicon replication, and demonstrated a diffuse punctate staining concordant with that described previously for FMDV 3A (García-Briones *et al.*, 2006; González-Magaldi *et al.*, 2012, 2014; O'Donnell *et al.*, 2001).

Replication-defective 3A mutations can be complemented *in trans*

Previous studies with FMDV and other picornaviruses have demonstrated that certain NS protein functions can be rescued *in trans* by co-expression with a replication-competent helper virus or replicon (García-Arriaza *et al.*, 2005; Giachetti *et al.*, 1992; Teterina *et al.*, 1995; Tiley *et al.*, 2003; Towner *et al.*, 1998). All of the 3A transposon insertions identified in this study were located within the 3A C-terminus, downstream of the predicted transmembrane domain, and the majority were replication-competent in BHK-21 cells. The one exception was the single replication-defective 3A transposon insertion site identified, 3A341, which was isolated after transfection with the higher amount of the mutant replicon library, along with

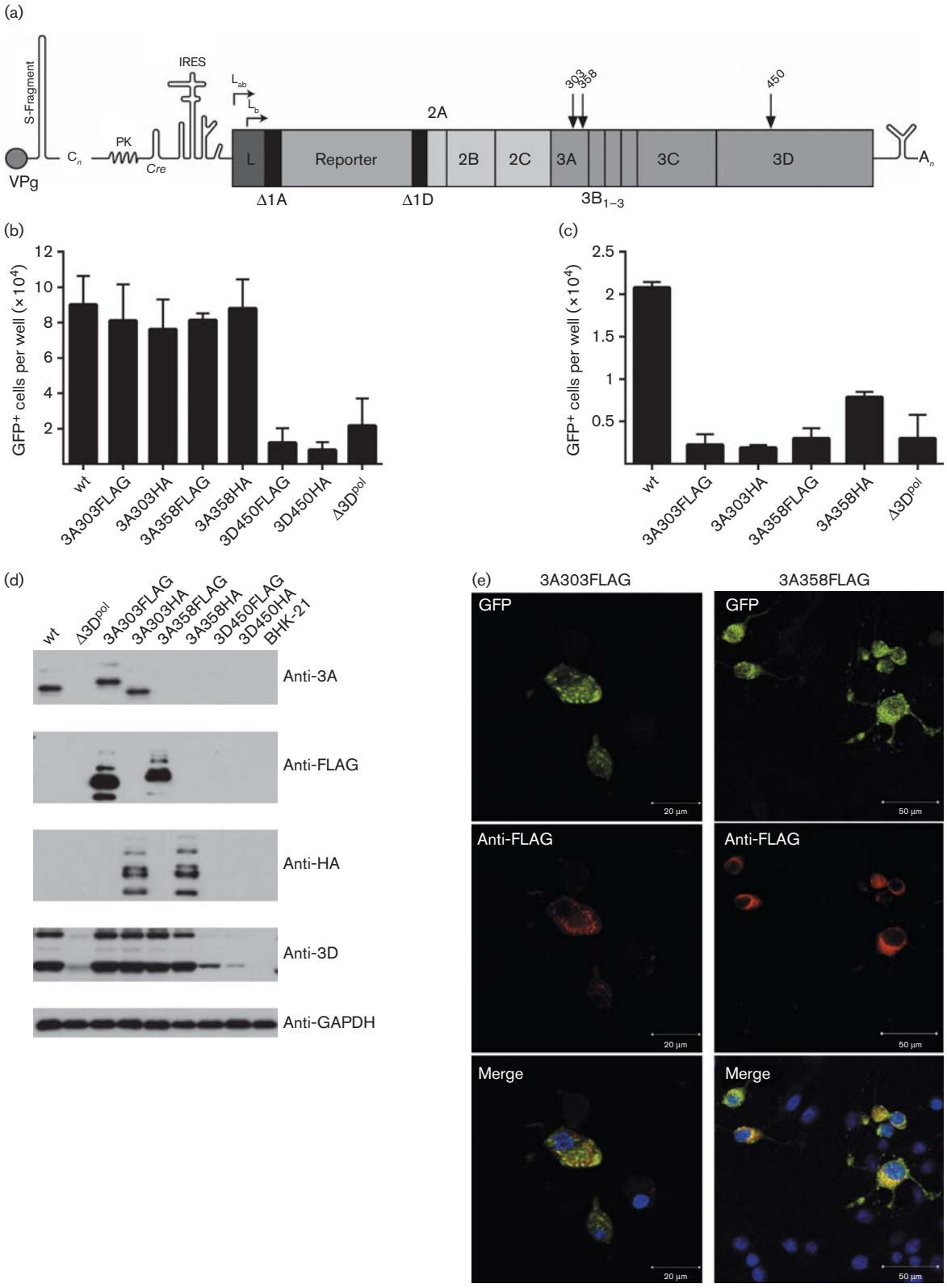

Fig. 3. Replication of epitope-tagged FMDV replicons. (a) Schematic of the FMDV replicon genome showing the positions of the inserted 3A or 3D epitope tags. (b, c) BHK-21 (b) or MDBK (c) cells seeded into 24-well plates were allowed to adhere for 16 h before transfection with replicon transcripts containing epitope tags using Lipofectin reagent. Wt GFP–PAC replicon (wt) and polymerase knockout ($\Delta 3D^{pol}$) constructs were included as controls. GFP expression was monitored hourly using an

IncuCyte Zoom Dual Colour FLR and analysed using the integrated software. The data shown represent GFP-positive cells per well at 8 h post-transfection ($n=2$, mean ± SEM). (d) BHK-21 cells were transfected with epitope-tagged 3A and 3D constructs in addition to controls. Protein lysates were prepared at 8 h post-transfection and probed by Western blotting for FLAG and HA expression plus 3A and 3D NS proteins and glyceraldehyde 3-phosphate dehydrogenase (GAPDH) as a loading control. (e) BHK-21 cells seeded onto glass coverslips were fixed in formaldehyde at 8 h post-transfection before being stained for anti-FLAG (red), GFP expression (green) and cell nuclei (DAPI; blue). Images were captured by confocal microscopy.

multiple other replication-defective $3C^{pro}$ and $3D^{pol}$ insertions. We hypothesized that selection using this higher concentration of transposon library was fostering an environment favourable for replication-defective insertions to be replicated *in trans* due to co-transfection with replication-competent genomes in the library.

To investigate this possibility, the replication-defective 3A341 transposon insertion was introduced into a replicon construct in which the GFP–PAC reporter cassette had been replaced by mCherry red fluorescent protein (F. Tulloch, G. Luke, J. Nicholson and M. D. Ryan, unpublished data). In addition, two negative-control replicons were generated containing either a double point mutation in the $3D^{pol}$ active site GDD motif ($3D^{pol}$GNN) or the same $3D^{pol}$ deletion as used previously ($\Delta 3D^{pol}$). Equivalent 'helper' replicon constructs were generated containing the GFP reporter gene from *Ptilosarcus* (ptGFP) in place of mCherry (F. Tulloch, G. Luke, J. Nicholson and M. D. Ryan, unpublished data), allowing discrimination of replication between the replication-defective mCherry construct and the 'helper' replicon. We theorized that the use of 'helper' replicons would allow expression of wt 3A from the native precursor(s) with the level and timing of protein expression balanced with that of the mutant replicon.

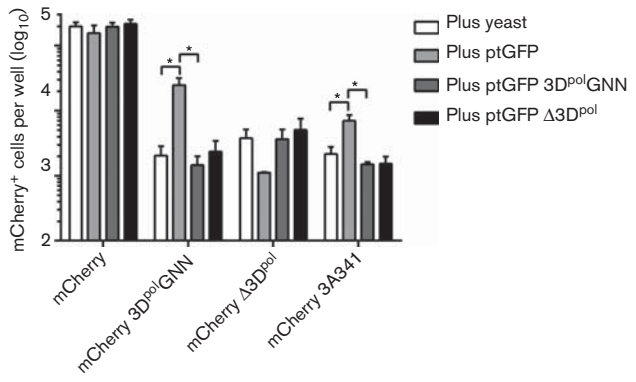

Fig. 4. Replication-defective 3A insertions can be complemented *in trans.* BHK-21 cells seeded into 24-well plates were allowed to adhere for 16 h before co-transfection using Lipofectin reagent with mCherry replicons containing either a $3D^{pol}$ or 3A replication-defective mutation or the wt control, and a wt (ptGFP) or polymerase knockout helper replicon expressing ptGFP (ptGFP $3D^{pol}$GNN and ptGFP $\Delta 3D^{pol}$) or yeast tRNA as a negative control. Both mCherry and ptGFP expression were monitored hourly using an IncuCyte Zoom Dual Colour FLR and analysed using the integrated software. The data shown represent mCherry-positive cells per well at 8 h post-transfection ($n=3$, mean ± SEM, $^*P<0.05$).

The ptGFP replicons were subsequently assessed for their ability to support replication of the mCherry replicons bearing replication-defective mutations (Fig. 4). For the replicon bearing the replication-defective mutation 3A341, *trans*-complementation was observed when this was co-transfected with the wt ptGFP 'helper' construct, with an approximate twofold significant increase in mCherry expression. Neither of the replication-defective polymerase constructs (ptGFP $3D^{pol}$GNN or ptGFP $\Delta 3D^{pol}$) was able to rescue the 3A mutant. However, the $3D^{pol}$ active site point mutant construct could itself be efficiently rescued *in trans* by co-transfection with a wt helper replicon. Interestingly, however, the mutant construct bearing a replication-defective $3D^{pol}$ deletion (mCherry–$\Delta 3D^{pol}$) was not rescued by any of the 'helper' replicons, with only a small but non-significant decrease in mCherry fluorescence observed upon co-transfection with the wt ptGFP replicon. Thus, these data would suggest that, whereas both 3A and $3D^{pol}$ can be complemented *in trans*, not all functions of $3D^{pol}$ can be rescued by co-transfection, indicating some *cis* preferential functions of certain NS proteins.

DISCUSSION

Understanding the replication of positive-strand RNA viruses is key to the development of novel therapeutic strategies. Despite over 50 years of intense study, relatively little is known about the molecular interactions within the picornavirus RNA replication complex, and the functions of some viral proteins have not yet been fully elucidated.

Here, we conducted transposon insertional mutagenesis of the FMDV NS polyprotein to find some of the locations within individual NS proteins that could accept insertions of epitope tags while maintaining replicon replication. Selection from the transposon-mutated replicon pool was conducted at both low and three times higher concentrations of the replicon library RNA. At both concentrations, replication-competent insertion sites were readily identified in 3A, with 16 separate 3A insertions identified across the two concentrations. Notably, all insertion sites were located within the C-terminal unstructured region, with the most N-terminal insertion occurring

immediately following the terminal residue of the predicted transmembrane domain (Fig. S3). It is remarkable that, for a protein of 459 nt, no insertions were identified in the first 229 nt, strongly implicating the N-terminal half of the protein as essential for viral RNA replication. Furthermore, transposon mutagenesis of the poliovirus genome by Teterina *et al.* (2011a) only isolated functional 3A insertion sites within the first 11 aa of the protein and not within the N-terminal α-helical and hydrophobic domains, further highlighting the importance of these structures in picornavirus replication. The N-terminal portion of FMDV 3A is predicted to contain two α-helices involved in 3A homodimerization followed by a hydrophobic transmembrane domain spanning residues ~59–76 (González-Magaldi *et al.*, 2012). In comparison with the N-terminal region, the C-terminal portion of FMDV 3A is relatively non-conserved and is extended by some 60 aa compared with most other picornaviruses. Mutations, insertions and deletions within the C-terminal region of 3A have implicated its importance for pathogenicity and host range, with natural viral isolates with large deletions in this region having been identified (such as aa 85–102, 93–102 and 133–143) (Knowles *et al.*, 2001; O'Donnell *et al.*, 2001; Pacheco *et al.*, 2003, 2013). Deletion of aa 93–102 of 3A has been observed in natural isolates of FMDV, and this correlates with an attenuated phenotype in cattle, but normal porcine pathogenicity and replication both *in vitro* and *in vivo* (Beard & Mason, 2000; Knowles *et al.*, 2001; Li *et al.*, 2010, 2011). However, it is not clear whether the 3A deletion alone is responsible for this phenotype and the molecular basis for the host-specific restriction of replication is unknown. It has been demonstrated by immunofluorescent and fluorescence recovery after photobleaching (FRAP) studies that deletions within either the N- or C-terminal regions of 3A can increase protein mobility and alter the cellular distribution in the absence of virus replication, an observation potentially related to the interaction of 3A with the cellular protein DCTN3, which has been implicated in the pathogenicity phenotype in cattle (Gladue *et al.*, 2014; González-Magaldi *et al.*, 2014). Host-cell restriction of 3A is of particular significance, as some of the 3A insertions tested allowed replication in BHK-21 cells, while restricting replication in the MDBK bovine cell line. Further investigation is warranted into the 3A-mediated host-cell phenotype, in particular the C-terminal unstructured half of the protein, and particular care must be taken when choosing the cellular context for understanding the molecular basis of virus replication.

Transposon insertions were identified within all three copies of 3B. However, previous studies have suggested the possibility of redundancy within the repeated 3B proteins, and it is not known at present whether 3B proteins bearing insertions retain the function of the protein (Arias *et al.*, 2010; Falk *et al.*, 1992). A tagged poliovirus has been generated containing an 8 aa HA tag after aa 17 of 3B, which displayed wt growth properties, suggesting that some of the 3B insertion sites identified here may retain protein function. Interestingly, however, the insertions tested in both $3B_1$ and $3B_3$ abolished replication in the bovine cell line MDBK, while maintaining good replication in BHK-21 cells. In contrast, the insertion in $3B_2$ demonstrated good replication in both cell lines, potentially suggesting a role of the various 3B proteins in regulating host-cell restriction.

One striking observation was the difference in the numbers of $3C^{pro}$ and $3D^{pol}$ insertions identified using a low versus a high concentration of the mutated library for selection. At the lower library concentration, no insertional sites were identified within $3C^{pro}$, and a single transposon insertion was identified within $3D^{pol}$ (3D450), which replicated efficiently in both BHK-21 and MDBK cells. This insertion is located in an unstructured region at the end of α5 on the outside of the finger domain (Fig. S4), which, despite the conservation between picornavirus $3D^{pol}$ polymerases, was not identified in a transposon mutagenesis study of poliovirus (Teterina *et al.*, 2011a). In contrast, selection at the higher RNA concentration readily yielded $3C^{pro}$ and $3D^{pol}$ insertions, all of which were found to completely eliminate replicon replication in isolation, as did the only replication-defective 3A insertion site identified (3A341). However, it must be noted that the observed preference for $3C^{pro}$ and $3D^{pol}$ insertions (at the higher concentration of library RNA) may be an unintentional consequence of the non-exhaustive screening approach used in selecting a limited number of colonies at each RNA concentration from a relatively large transposon library.

The frequencies at which replication-defective insertions were identified using a high RNA concentration led us to hypothesize that transfection of greater amounts of replicon RNA provided conditions in which replication-defective genomes were being maintained or replicated *in trans*, by coincidental co-transfection with genomes containing replication-permissive insertions. In accordance with this hypothesis, replication of a construct bearing the lethal replication-defective 3A insertion was rescued by simultaneous co-transfection of a wt 'helper' replicon. *Trans*-complementation of replication-defective NS protein mutations has been described within some NS proteins of picornaviruses including poliovirus 3A (Giachetti *et al.*, 1992; Teterina *et al.*, 1995; Towner *et al.*, 1998) and some FMDV proteins (García-Arriaza *et al.*, 2005; Tiley *et al.*, 2003). However, to the best of our knowledge, this is the first study to demonstrate rescue *in trans* of a replication-defective FMDV 3A mutation.

Due to the limited structural information on the C-terminal domain of 3A, it is hard to speculate why the 3A341 insertion renders the replicon replication-defective. The observation that this replication-defective lesion can be complemented *in trans* and that insertions at positions 3A339 and 3A342 were tolerated in both hamster and bovine cells suggests a disruption in 3A protein function, as opposed to effects at the RNA level. Further characterization of the 3A341 insertion may be valuable in yielding

information on the function of the FMDV 3A C-terminal region.

Having identified functional transposon insertion sites, we generated replicon constructs containing epitope tags in either 3A or $3D^{pol}$. A FLAG or HA tag was successfully inserted into two separate locations of 3A to yield replication-competent replicons that could be characterized by Western blotting and immunofluorescence analysis. Incorporation of either tag into the 3A358 position abolished recognition by the anti-3A 2C2 mAb, possibly due to disruption of the mAb epitope or disruption of the native 3A C-terminal folding. Incorporation of either tag into the 3A303 position allowed recognition to be maintained for the antibody, but resulted in slight changes of 3A mobility by SDS-PAGE, particularly in the case of the FLAG epitope, possibly due to the change in the local charge environment in this unstructured region. Insertions of functional epitope tags have been reported previously in the N-terminal region of poliovirus 3A, albeit with some deleterious effects on replication, and within the C-terminal region of FMDV 3A at similar locations as described here (Li *et al.*, 2012; Ma *et al.*, 2015; Teterina *et al.*, 2011b). However, despite the success of epitope tagging of 3A in this study, $3D^{pol}$ did not tolerate the insertion of epitope tags at the single replication-competent transposon insertion site identified, presumably due to the nature of the sequence of the epitope insertion at this location.

In comparison with P3, few insertions were identified within P2, either in this study, which identified only two replication-defective insertions in 2C, or in a previous transposon mutagenesis study of poliovirus where only one replication-competent insertion was identified at the N-terminus of 2B (Teterina *et al.*, 2011a). Together, these data suggest that P2 is relatively less amenable for mutation or modification when compared with P3, and a more focused study using transposon mutation of P2 alone may be required to discover replication-competent insertions in the FMDV 2B and 2C NS proteins. However, the methodologies used to identify insertions in both this and the previous study by Tererina *et al.* (2011a) were non-exhaustive and it is therefore possible that tolerated P2 insertions could be identified using alternative methodologies, such as next-generation sequencing.

In conclusion, we used random transposon-mediated mutagenesis to identify replication-tolerant insertion sites within the P3 region of the FMDV NS polyprotein and exploited these sites for the incorporation of epitope tags, which will be invaluable for downstream studies. Furthermore, selection using high concentrations of mutagenized replicon RNA enabled the identification of replication-defective insertions that could be rescued *in trans*. Further investigation of such replication-defective mutations is ongoing and may yield insights into the mechanisms of picornaviral RNA replication.

METHODS

Cells lines. BHK-21 and MDBK cells were obtained from the ATCC (LGC Standard) and maintained in Dulbecco's modified Eagle's medium with glutamine (Sigma-Aldrich) supplemented with 10 % FCS, 50 U penicillin ml^{-1} and 50 μg streptomycin ml^{-1}.

Plasmid constructs. The FMDV replicon plasmid constructs pGFP-PAC and pGFP-PAC-Δ$3D^{pol}$ polymerase knockout control have been described previously (Tulloch *et al.*, 2014).

Generation of the transposon-mutated replicon library first required transfer of the FMDV NS polyprotein coding region into a subcloning vector for mutagenesis. Therefore, the *Xma*I–*Bam*HI fragment from pGFP-PAC was transferred to *Xma*I/*Bam*HI-digested pUC18 (Invitrogen) to regenerate pUC-2A-3D. The transposon mutagenesis system Mutation Generation System kit (Life Technologies) was employed following the manufacturer's instructions, for transposition of a chloramphenicol-resistant transposon, on construct pUC-2A-3D to generate the plasmid library pUC-2A-3D-TnC. Here, each plasmid contained on average a single chloramphenicol-resistant transposon insertion. Mutagenized clones were transformed in ElecoTen Ultra-competent cells (Stratagene), selected for resistance to chloramphenicol plus kanamycin, and total colonies were collected. The library was estimated to contain over 20 000 clones. This library was subsequently digested with *Xma*I and *Bam*HI and the resulting fragment of approximately 4.7 kb was cloned back into pGFP-PAC and selected against chloramphenicol and ampicillin to remove the wt replicon and so create the replicon library pGFP-PAC-TnC. The library pGFP-PAC-TnC was digested with *Not*I to remove the chloramphenicol resistance cassette, and re-ligated to make pGFP-PAC-Tn, a replicon library containing 15 nt insertions randomly located across the FMDV NS polyprotein coding region.

To introduce individual transposon insertions into the replicon plasmid, the *Xma*I–*Bam*HI fragment from pGFP-PAC was replaced by an equivalent *Xma*I–*Bam*HI fragment obtained from the cloned products derived from the initial transposon selection experiment.

***In vitro* transcription.** Replicon plasmid DNA (5 μg) was linearized with *Hpa*I (NEB) or *Asc*I (NEB), as appropriate, purified by phenol/chloroform extraction, ethanol precipitated and redissolved in RNase-free water. The linear DNA was used in a 50 μl *in vitro* transcription reaction containing transcription buffer and BSA, and treated with RNasecure reagent (Ambion) following the manufacturer's recommendation, before the addition of 40 U T7 polymerase (NEB), 50 U RNaseOut (Invitrogen) and 8 mM rNTPs (Roche). The *in vitro* transcription reaction was incubated at 32 °C for 4 h after which 2.5 U RQ1 DNase (Promega) was added, followed by incubation at 37 °C for 30 min before the RNA was recovered with an RNA Clean & Concentrator-25 spin column (Zymo Research) following the manufacturer's instructions. Transcript integrity was assessed by MOPS/formaldehyde gel electrophoresis prior to transfection.

Cell transfection and fluorescent reporter assays. BHK-21 and MDBK cells were seeded into tissue culture plates at 5×10^4 and 6.25×10^4 cells cm^{-2}, respectively and allowed to adhere for 16 h. Immediately prior to transfection, cells were washed briefly in PBS and the medium replaced with 100 μl minimal essential medium (Invitrogen) cm^{-2} supplemented with 10 % FCS, 50 U penicillin ml^{-1}, 50 μg streptomycin ml^{-1}, 1 × non-essential amino acids and 2 mM glutamine. Duplicate wells were transfected with replicon transcripts using Escort I transfection reagent (Sigma) or Lipofectin (Life Technologies) as indicated, following the manufacturer's instructions, using 0.25 or 0.5 μg of total RNA cm^{-2}, respectively. For co-transfections, equal amounts of the two RNA transcripts were transfected simultaneously.

Fluorescent protein expression and live cell imaging were analysed using an IncuCyte Dual Colour Zoom FLR (Essen BioScience) within a 37 °C humidified CO_2 incubator scanning hourly up to 24 h post-transfection, collecting multiple images per well. Images were analysed using the associated Zoom software with the integrated algorithm measuring fluorescent object counts per well as described previously (Forrest *et al.*, 2014; Tulloch *et al.*, 2014). The data are presented to show GFP expression at 8 h post-transfection as a measure of maximum replication.

Isolation of transposon insertions. Following BHK-21 cell transfection of *in vitro*-transcribed replicon RNA or replicon library RNA, cells were detached by trypsin and washed once in ice-cold PBS. Total RNA was extracted from the cell pellet using TRIzol reagent (Life Technologies) following the manufacturer's protocol. Total RNA was treated with RQ1-DNase (Promega) and the FMDV cDNA amplified using Superscript II (Life Technologies) following the manufacturer's protocol. FMDV genomes were amplified using Phusion High-Fidelity DNA polymerase (NEB) and blunt-end ligated into pCRBlunt. Individual colonies were isolated and the location of transposon insertions was identified by DNA sequencing.

Western blotting. Immunoblotting was carried out as described previously (Forrest *et al.*, 2014). Briefly, cells were washed in PBS, detached with trypsin and washed in PBS before lysis in radioimmunoprecipitation assay buffer [0.1 % SDS, 0.5 % sodium deoxycholate, 1 % NP-40, 150 mM sodium chloride, 50 mM Tris/HCl (pH 8.0), 1 mM EDTA] supplemented with 2 × complete protease inhibitor (Roche) and incubated on ice for 5 min before clarification by centrifugation. Cell lysates were separated by SDS-PAGE using a miniProtean gel system (Bio-Rad), followed by transfer to PVDF membrane (Bio-Rad) using an XCell *SureLock* Mini-Cell wet transfer apparatus (Life Technologies). Membranes were blocked with 10 % dried milk, 0.1 % Tween-20 (Sigma-Aldrich) in Tris-buffered saline. The primary antibodies used were rabbit anti-3D 397 polyclonal antibody, mouse anti-3A 2C2 mAb (from Professor Francisco Sobrino, Centro De Biologia Molecular Severo Ochoa, Madrid, Spain), mouse anti-FLAG M2 (Sigma-Aldrich) and mouse anti-HA (Sigma-Aldrich), and were detected with anti-mouse–HRP or anti-rabbit–HRP secondary antibodies (Sigma-Aldrich), as appropriate.

Confocal microscopy. BHK-21 cells seeded onto glass coverslips were transfected with *in vitro* transcripts, fixed at the indicated time points with 4 % paraformaldehyde, washed in PBS and permeabilized in saponin buffer (1 % saponin, 10 % FCS, 0.1 % sodium azide) for 1 h at 4 °C. Primary and secondary antibodies were incubated in saponin buffer for 2 h at room temperature with three washes in saponin buffer between steps. Primary antibody anti-FLAG M2 (Sigma-Aldrich) was detected with anti-mouse–Alexa Fluor 568 (Life Technologies) secondary antibody. Following a final wash in PBS, the coverslips were mounted in VECTASHIELD mounting medium with DAPI (Vector Laboratories) and images were captured using a Zeiss LSM-700 confocal microscope.

ACKNOWLEDGEMENTS

We would like to thank Professor Sobrino at the Centro De Biologia Molecular in Madrid for the generous gift of antibodies, Dr Martin Stacey plus colleagues at the University of Leeds and Dr Christopher McCormick at the University of Southampton for helpful comments on this manuscript. This work was funded by the BBSRC (grants BB/F01614X/1 and BB/K003801/1).

REFERENCES

Arias, A., Perales, C., Escarmís, C. & Domingo, E. (2010). Deletion mutants of VPg reveal new cytopathology determinants in a picornavirus. *PLoS One* **5**, e10735.

Beard, C. W. & Mason, P. W. (2000). Genetic determinants of altered virulence of Taiwanese foot-and-mouth disease virus. *J Virol* **74**, 987–991.

Belsham, G. J. & Brangwyn, J. K. (1990). A region of the 5′ noncoding region of foot-and-mouth disease virus RNA directs efficient internal initiation of protein synthesis within cells: involvement with the role of L protease in translational control. *J Virol* **64**, 5389–5395.

Birtley, J. R., Knox, S. R., Jaulent, A. M., Brick, P., Leatherbarrow, R. J. & Curry, S. (2005). Crystal structure of foot-and-mouth disease virus 3C protease. New insights into catalytic mechanism and cleavage specificity. *J Biol Chem* **280**, 11520–11527.

Brune, W., Ménard, C., Hobom, U., Odenbreit, S., Messerle, M. & Koszinowski, U. H. (1999). Rapid identification of essential and nonessential herpesvirus genes by direct transposon mutagenesis. *Nat Biotechnol* **17**, 360–364.

Carrillo, C., Tulman, E. R., Delhon, G., Lu, Z., Carreno, A., Vagnozzi, A., Kutish, G. F. & Rock, D. L. (2005). Comparative genomics of foot-and-mouth disease virus. *J Virol* **79**, 6487–6504.

Clarke, B. E., Brown, A. L., Currey, K. M., Newton, S. E., Rowlands, D. J. & Carroll, A. R. (1987). Potential secondary and tertiary structure in the genomic RNA of foot and mouth disease virus. *Nucleic Acids Res* **15**, 7067–7079.

de Felipe, P., Hughes, L. E., Ryan, M. D. & Brown, J. D. (2003). Co-translational, intraribosomal cleavage of polypeptides by the foot-and-mouth disease virus 2A peptide. *J Biol Chem* **278**, 11441–11448.

Doedens, J. R. & Kirkegaard, K. (1995). Inhibition of cellular protein secretion by poliovirus proteins 2B and 3A. *EMBO J* **14**, 894–907.

Donnelly, M. L., Hughes, L. E., Luke, G., Mendoza, H., ten Dam, E., Gani, D. & Ryan, M. D. (2001). The 'cleavage' activities of foot-and-mouth disease virus 2A site-directed mutants and naturally occurring '2A-like' sequences. *J Gen Virol* **82**, 1027–1041.

Escarmís, C., Dopazo, J., Dávila, M., Palma, E. L. & Domingo, E. (1995). Large deletions in the 5′-untranslated region of foot-and-mouth disease virus of serotype C. *Virus Res* **35**, 155–167.

Falk, M. M., Sobrino, F. & Beck, E. (1992). VPg gene amplification correlates with infective particle formation in foot-and-mouth disease virus. *J Virol* **66**, 2251–2260.

Ferrer-Orta, C., Arias, A., Perez-Luque, R., Escarmís, C., Domingo, E. & Verdaguer, N. (2004). Structure of foot-and-mouth disease virus RNA-dependent RNA polymerase and its complex with a template-primer RNA. *J Biol Chem* **279**, 47212–47221.

Ferrer-Orta, C., Arias, A., Agudo, R., Pérez-Luque, R., Escarmís, C., Domingo, E. & Verdaguer, N. (2006). The structure of a protein primer-polymerase complex in the initiation of genome replication. *EMBO J* **25**, 880–888.

Ferrer-Orta, C., Agudo, R., Domingo, E. & Verdaguer, N. (2009). Structural insights into replication initiation and elongation processes by the FMDV RNA-dependent RNA polymerase. *Curr Opin Struct Biol* **19**, 752–758.

Forrest, S., Lear, Z., Herod, M. R., Ryan, M., Rowlands, D. J. & Stonehouse, N. J. (2014). Inhibition of the foot-and-mouth disease virus subgenomic replicon by RNA aptamers. *J Gen Virol* **95**, 2649–2657.

Forss, S. & Schaller, H. (1982). A tandem repeat gene in a picornavirus. *Nucleic Acids Res* **10**, 6441–6450.

García-Arriaza, J., Domingo, E. & Escarmís, C. (2005). A segmented form of foot-and-mouth disease virus interferes with standard virus: a link between interference and competitive fitness. *Virology* **335**, 155–164.

García-Briones, M., Rosas, M. F., González-Magaldi, M., Martín-Acebes, M. A., Sobrino, F. & Armas-Portela, R. (2006). Differential distribution of non-structural proteins of foot-and-mouth disease virus in BHK-21 cells. *Virology* **349**, 409–421.

Giachetti, C., Hwang, S. S. & Semler, B. L. (1992). cis-acting lesions targeted to the hydrophobic domain of a poliovirus membrane protein involved in RNA replication. *J Virol* **66**, 6045–6057.

Gladue, D. P., O'Donnell, V., Baker-Bransetter, R., Pacheco, J. M., Holinka, L. G., Arzt, J., Pauszek, S., Fernandez-Sainz, I., Fletcher, P. & other authors (2014). Interaction of foot-and-mouth disease virus nonstructural protein 3A with host protein DCTN3 is important for viral virulence in cattle. *J Virol* **88**, 2737–2747.

González-Magaldi, M., Postigo, R., de la Torre, B. G., Vieira, Y. A., Rodríguez-Pulido, M., López-Viñas, E., Gómez-Puertas, P., Andreu, D., Kremer, L. & other authors (2012). Mutations that hamper dimerization of foot-and-mouth disease virus 3A protein are detrimental for infectivity. *J Virol* **86**, 11013–11023.

González-Magaldi, M., Martín-Acebes, M. A., Kremer, L. & Sobrino, F. (2014). Membrane topology and cellular dynamics of foot-and-mouth disease virus 3A protein. *PLoS One* **9**, e106685.

Grubman, M. J., Zellner, M., Bablanian, G., Mason, P. W. & Piccone, M. E. (1995). Identification of the active-site residues of the 3C proteinase of foot-and-mouth disease virus. *Virology* **213**, 581–589.

King, A. M., Sangar, D. V., Harris, T. J. & Brown, F. (1980). Heterogeneity of the genome-linked protein of foot-and-mouth disease virus. *J Virol* **34**, 627–634.

Knowles, N. J., Davies, P. R., Henry, T., O'Donnell, V., Pacheco, J. M. & Mason, P. W. (2001). Emergence in Asia of foot-and-mouth disease viruses with altered host range: characterization of alterations in the 3A protein. *J Virol* **75**, 1551–1556.

Li, S., Gao, M., Zhang, R., Song, G., Song, J., Liu, D., Cao, Y., Li, T., Ma, B. & other authors (2010). A mutant of infectious Asia 1 serotype foot-and-mouth disease virus with the deletion of 10-amino-acid in the 3A protein. *Virus Genes* **41**, 406–413.

Li, S., Gao, M., Zhang, R., Song, G., Song, J., Liu, D., Cao, Y., Li, T., Ma, B. & other authors (2011). A mutant of Asia 1 serotype of Foot-and-mouth disease virus with the deletion of an important antigenic epitope in the 3A protein. *Can J Microbiol* **57**, 169–176.

Li, P., Bai, X., Cao, Y., Han, C., Lu, Z., Sun, P., Yin, H. & Liu, Z. (2012). Expression and stability of foreign epitopes introduced into 3A nonstructural protein of foot-and-mouth disease virus. *PLoS One* **7**, e41486.

López de Quinto, S. & Martínez-Salas, E. (1997). Conserved structural motifs located in distal loops of aphthovirus internal ribosome entry site domain 3 are required for internal initiation of translation. *J Virol* **71**, 4171–4175.

López de Quinto, S., Sáiz, M., de la Morena, D., Sobrino, F. & Martínez-Salas, E. (2002). IRES-driven translation is stimulated separately by the FMDV 3′-NCR and poly(A) sequences. *Nucleic Acids Res* **30**, 4398–4405.

Ma, X., Li, P., Sun, P., Bai, X., Bao, H., Lu, Z., Fu, Y., Cao, Y., Li, D., Chen, Y., Qiao, Z. & Liu, Z. (2015). Construction and characterization of 3A-epitope-tagged foot-and-mouth disease virus. *Infect Genet Evol* **31**, 17–24.

Mason, P. W., Bezborodova, S. V. & Henry, T. M. (2002). Identification and characterization of a *cis*-acting replication element (*cre*) adjacent to the internal ribosome entry site of foot-and-mouth disease virus. *J Virol* **76**, 9686–9694.

Mason, P. W., Grubman, M. J. & Baxt, B. (2003). Molecular basis of pathogenesis of FMDV. *Virus Res* **91**, 9–32.

McMahon, C. W., Traxler, B., Grigg, M. E. & Pullen, A. M. (1998). Transposon-mediated random insertions and site-directed mutagenesis prevent the trafficking of a mouse mammary tumor virus superantigen. *Virology* **243**, 354–365.

Moffat, K., Howell, G., Knox, C., Belsham, G. J., Monaghan, P., Ryan, M. D. & Wileman, T. (2005). Effects of foot-and-mouth disease virus nonstructural proteins on the structure and function of the early secretory pathway: 2BC but not 3A blocks endoplasmic reticulum-to-Golgi transport. *J Virol* **79**, 4382–4395.

Moffat, K., Knox, C., Howell, G., Clark, S. J., Yang, H., Belsham, G. J., Ryan, M. & Wileman, T. (2007). Inhibition of the secretory pathway by foot-and-mouth disease virus 2BC protein is reproduced by coexpression of 2B with 2C, and the site of inhibition is determined by the subcellular location of 2C. *J Virol* **81**, 1129–1139.

Möhl, B. S., Böttcher, S., Granzow, H., Fuchs, W., Klupp, B. G. & Mettenleiter, T. C. (2010). Random transposon-mediated mutagenesis of the essential large tegument protein pUL36 of pseudorabies virus. *J Virol* **84**, 8153–8162.

Nayak, A., Goodfellow, I. G. & Belsham, G. J. (2005). Factors required for the uridylylation of the foot-and-mouth disease virus 3B1, 3B2, and 3B3 peptides by the RNA-dependent RNA polymerase ($3D^{pol}$) in vitro. *J Virol* **79**, 7698–7706.

O'Donnell, V. K., Pacheco, J. M., Henry, T. M. & Mason, P. W. (2001). Subcellular distribution of the foot-and-mouth disease virus 3A protein in cells infected with viruses encoding wild-type and bovine-attenuated forms of 3A. *Virology* **287**, 151–162.

Pacheco, J. M., Henry, T. M., O'Donnell, V. K., Gregory, J. B. & Mason, P. W. (2003). Role of nonstructural proteins 3A and 3B in host range and pathogenicity of foot-and-mouth disease virus. *J Virol* **77**, 13017–13027.

Pacheco, J. M., Gladue, D. P., Holinka, L. G., Arzt, J., Bishop, E., Smoliga, G., Pauszek, S. J., Bracht, A. J., O'Donnell, V. & other authors (2013). A partial deletion in non-structural protein 3A can attenuate foot-and-mouth disease virus in cattle. *Virology* **446**, 260–267.

Paul, A. V., van Boom, J. H., Filippov, D., Wimmer, E. & Protein-primed, R. N. A. (1998). synthesis by purified poliovirus RNA polymerase. *Nature* **393**, 280–284.

Paul, A. V., Yin, J., Mugavero, J., Rieder, E., Liu, Y. & Wimmer, E. (2003). A "slide-back" mechanism for the initiation of protein-primed RNA synthesis by the RNA polymerase of poliovirus. *J Biol Chem* **278**, 43951–43960.

Remenyi, R., Qi, H., Su, S. Y., Chen, Z., Wu, N. C., Arumugaswami, V., Truong, S., Chu, V., Stokelman, T. & other authors (2014). A comprehensive functional map of the hepatitis C virus genome provides a resource for probing viral proteins. *MBio* **5**, e01469–14.

Rodríguez, P. L. & Carrasco, L. (1993). Poliovirus protein 2C has ATPase and GTPase activities. *J Biol Chem* **268**, 8105–8110.

Rodríguez Pulido, M., Sobrino, F., Borrego, B. & Sáiz, M. (2009). Attenuated foot-and-mouth disease virus RNA carrying a deletion in the 3′ noncoding region can elicit immunity in swine. *J Virol* **83**, 3475–3485.

Rowlands, D. J., Harris, T. J. & Brown, F. (1978). More precise location of the polycytidylic acid tract in foot and mouth disease virus RNA. *J Virol* **26**, 335–343.

Ryan, M. D. & Drew, J. (1994). Foot-and-mouth disease virus 2A oligopeptide mediated cleavage of an artificial polyprotein. *EMBO J* **13**, 928–933.

Ryan, M. D. & Flint, M. (1997). Virus-encoded proteinases of the picornavirus super-group. *J Gen Virol* **78**, 699–723.

Sáiz, M., Gómez, S., Martínez-Salas, E. & Sobrino, F. (2001). Deletion or substitution of the aphthovirus 3′ NCR abrogates infectivity and virus replication. *J Gen Virol* **82**, 93–101.

Teterina, N. L., Zhou, W. D., Cho, M. W. & Ehrenfeld, E. (1995). Inefficient complementation activity of poliovirus 2C and 3D proteins for rescue of lethal mutations. *J Virol* **69**, 4245–4254.

Teterina, N. L., Levenson, E. A. & Ehrenfeld, E. (2010). Viable polioviruses that encode 2A proteins with fluorescent protein tags. *J Virol* **84**, 1477–1488.

Teterina, N. L., Lauber, C., Jensen, K. S., Levenson, E. A., Gorbalenya, A. E. & Ehrenfeld, E. (2011a). Identification of tolerated insertion sites in poliovirus non-structural proteins. *Virology* **409**, 1–11.

Teterina, N. L., Pinto, Y., Weaver, J. D., Jensen, K. S. & Ehrenfeld, E. (2011b). Analysis of poliovirus protein 3A interactions with viral and cellular proteins in infected cells. *J Virol* **85**, 4284–4296.

Thorne, L., Bailey, D. & Goodfellow, I. (2012). High-resolution functional profiling of the norovirus genome. *J Virol* **86**, 11441–11456.

Tiley, L., King, A. M. & Belsham, G. J. (2003). The foot-and-mouth disease virus cis-acting replication element (*cre*) can be complemented in trans within infected cells. *J Virol* **77**, 2243–2246.

Towner, J. S., Mazanet, M. M. & Semler, B. L. (1998). Rescue of defective poliovirus RNA replication by 3AB-containing precursor polyproteins. *J Virol* **72**, 7191–7200.

Tulloch, F., Pathania, U., Luke, G. A., Nicholson, J., Stonehouse, N. J., Rowlands, D. J., Jackson, T., Tuthill, T., Haas, J. & other authors (2014). FMDV replicons encoding green fluorescent protein are replication competent. *J Virol Methods* **209**, 35–40.

Xia, H., Wang, P., Wang, G. C., Yang, J., Sun, X., Wu, W., Qiu, Y., Shu, T., Zhao, X. & other authors (2015). Human enterovirus nonstructural protein 2CATPase functions as both an RNA helicase and ATP-independent RNA chaperone. *PLoS Pathog* **11**, e1005067.